$B\to\pi\pi,K\pi$ decays in the QCD improved factorization approach

Taizo Muta,[1] Akio Sugamoto,[2] Mao-Zhi Yang,[1] and Ya-Dong Yang[2]
[1]*Physics Department, Hiroshima University, Higashi-Hiroshima, Hiroshima 739-8526, Japan*
[2]*Physics Department, Ochanomizu University, 2-1-1 Otsuka, Bunkyo-ku, Tokyo 112-8610, Japan*
(Received 5 June 2000; published 9 October 2000)

Motivated by recent measurements, we investigate $B\to\pi\pi,K\pi$ decay modes in the framework of QCD improved factorization, which was recently proposed by Beneke *et al.* We find that all the measured branching ratios are well accommodated in the reasonable parameter space except for $B\to K^0\pi^0$. We also discuss in detail the strong penguin contributions and the $\mathcal{O}(\alpha_s)$ corrections to the chirally enhanced terms. We find that the weak phase γ lies in the region $120°<\gamma<240°$, which is mainly constrained by $B\to\pi^-\pi^+$.

PACS number(s): 13.25.Hw, 12.15.Hh, 12.38.Bx

I. INTRODUCTION

It is well known that the theoretical description of nonleptonic B decays is an extreme challenge, due to the nonperturbative nature of both initial and final mesons. A good understanding of the B nonleptonic decays, or at least a reliable estimation, is the prerequisite for extracting meaningful implications from experimental data and for testing the standard model (SM). In past years, some advances have been made toward the goal, for example, in Refs. [1–3].

Recently, Beneke, Buchalla, Neubert, and Sachrajda [4] have presented a promising factorization formula for the charmless nonleptonic B decays. The basic object in the calculation of B charmless nonleptonic decays is the hadronic matrix element $\langle M_1(p_1)M_2(p_2)|\mathcal{O}_i|B(p)\rangle$, where $\mathcal{O}_i$ is the effective operator inducing the decay, M_1 is the final meson absorbing the light spectator quark from the B meson, and M_2 is another light meson flying fast from the b quark decay point as implied by $\mathcal{O}_i$. The light spectator quark is translated softly to M_1 and this effect could be taken to the nonperturbative form factor $F_{1,2}^{B\to M_1}$ unless it undergoes a hard interaction. The quark pair, forming M_2, ejected from b decay point carrying large energy of order of m_b will involve hard interaction, since soft gluon with momentum of order $\Lambda_{\rm QCD}$ will decouple from the quark pair at leading order in $\Lambda_{\rm QCD}/m_b$ in the heavy quark limit. The essence of the argument of Ref. [4] can be summarized by the improved factorization formula

$$\begin{aligned}\langle M_1(p_1)M_2(p_2)|\mathcal{O}_i|B(p)\rangle &= F^{B\to M_1}(M_2^2)\int_0^1 dx T_i^I(x)\phi_{M_2}(x)\\ &\quad+\int_0^1 dxdydz T_i^{II}(x,y,z)\phi_{M_1}(x)\phi_{M_2}(y)\phi_B(z),\end{aligned}\tag{1}$$

where $\phi_P(x)$ are the P meson's light-cone distribution amplitudes (DAs). The hard amplitudes $T_i^{\rm I,II}$ can be perturbatively expanded in $\alpha_s(m_b)$ and can be obtained from the calculations of the diagrams in Fig. 1. It is interesting to note that $T_i^{\rm I}$ would be unity and $T_i^{\rm II}$ would be absent at zeroth order of α_s in the formula of Eq. (1), then the naive factorization would be reproduced. Another consequence of Eq. (1) is that the final state interactions may be computable and appear to be the imaginary part of the hard scattering amplitudes.

In this work, we extend the formalism to $\overline{B}\to K\pi$ decays and recalculate $\overline{B}\to\pi\pi$ decays with electroweak penguin contributions. We also present detailed discussions about the strong penguin contributions and therefore we obtain the corrections to the chiral enhanced terms, which are found free of infrared divergence. We point out that there is large cancellation between the strong penguin hard scattering amplitudes and its contributions are small. Prospects of observing CP violation in those decay modes are also discussed.

II. CALCULATIONS

First we begin with the weak effective Hamiltonian $H_{\rm eff}$ for the $\Delta B=1$ transitions as [5]

$$\begin{aligned}\mathcal{H}_{\rm eff}=\frac{G_F}{\sqrt{2}}\Bigg[&V_{ub}V_{uq}^*\left(\sum_{i=1}^{2}C_iO_i^u+\sum_{i=3}^{10}C_iO_i+C_gO_g\right)\\ &+V_{cb}V_{cq}^*\left(\sum_{i=1}^{2}C_iO_i^c+\sum_{i=3}^{10}C_iO_i+C_gO_g\right)\Bigg].\end{aligned}\tag{2}$$

For convenience, we list the operators in $\mathcal{H}_{\rm eff}$ for $b\to q$ below:

$$\begin{aligned}O_1^u&=\overline{q}_\alpha\gamma^\mu Lu_\alpha\cdot\overline{u}_\beta\gamma_\mu Lb_\beta,\\ O_2^u&=\overline{q}_\alpha\gamma^\mu Lu_\beta\cdot\overline{u}_\beta\gamma_\mu Lb_\alpha,\\ O_1^c&=\overline{q}_\alpha\gamma^\mu Lc_\alpha\cdot\overline{c}_\beta\gamma_\mu Lb_\beta,\\ O_2^c&=\overline{q}_\alpha\gamma^\mu Lc_\beta\cdot\overline{c}_\beta\gamma_\mu Lb_\alpha,\\ O_3&=\overline{q}_\alpha\gamma^\mu Lb_\alpha\cdot\sum_{q'}\overline{q}'_\beta\gamma_\mu Lq'_\beta,\\ O_4&=\overline{q}_\alpha\gamma^\mu Lb_\beta\cdot\sum_{q'}\overline{q}'_\beta\gamma_\mu Lq'_\alpha,\end{aligned}\tag{3}$$

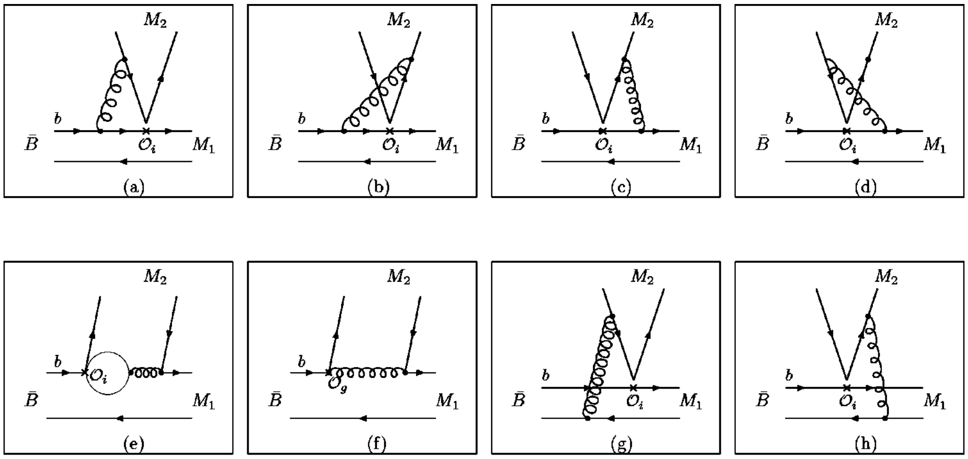

FIG. 1. Order α_s corrections to the hard scattering kernels T_i^{I} (a)–(f) and T_i^{II} (g),(h).

$$O_5=\overline{q}_\alpha\gamma^\mu L b_\alpha\cdot\sum_{q'}\overline{q}'_\beta\gamma_\mu R q'_\beta,$$

$$O_6=\overline{q}_\alpha\gamma^\mu L b_\beta\cdot\sum_{q'}\overline{q}'_\beta\gamma_\mu R q'_\alpha,$$

$$O_7=\frac{3}{2}\overline{q}_\alpha\gamma^\mu L b_\alpha\cdot\sum_{q'}e_{q'}\overline{q}'_\beta\gamma_\mu R q'_\beta,$$

$$O_8=\frac{3}{2}\overline{q}_\alpha\gamma^\mu L b_\beta\cdot\sum_{q'}e_{q'}\overline{q}'_\beta\gamma_\mu R q'_\alpha,$$

$$O_9=\frac{3}{2}\overline{q}_\alpha\gamma^\mu L b_\alpha\cdot\sum_{q'}e_{q'}\overline{q}'_\beta\gamma_\mu L q'_\beta,$$

$$O_{10}=\frac{3}{2}\overline{q}_\alpha\gamma^\mu L b_\beta\cdot\sum_{q'}e_{q'}\overline{q}'_\beta\gamma_\mu L q'_\alpha,$$

$$O_g=(g_s/8\pi^2)\, m_b\, \overline{d}_\alpha\, \sigma^{\mu\nu}\, R\, (\lambda^A_{\alpha\beta}/2)\, b_\beta G^A_{\mu\nu}.$$

Here $q=d,s$ and $(q'\epsilon\{u,d,s,c,b\})$. α and β are the $SU(3)$ color indices and $\lambda^A_{\alpha\beta}$, $A=1,\ldots,8$ are the Gell-Mann matrices; L and R are the left- and right-handed projection operators with $L=(1-\gamma_5)$, $R=(1+\gamma_5)$, and $G^A_{\mu\nu}$ denotes the gluonic field strength tensor. The Wilson coefficients evaluated at $\mu=m_b$ scale are [5]

$$\begin{aligned}
&C_1=1.082, \quad C_2=-0.185,\\
&C_3=0.014, \quad C_4=-0.035,\\
&C_5=0.009, \quad C_6=-0.041,\\
&C_7=-0.002/137, \quad C_8=0.054/137,\\
&C_9=-1.292/137, \quad C_{10}=-0.262/137,\\
&C_g=-0.143.
\end{aligned} \tag{4}$$

After direct calculations, we get the hard scattering for the decay modes listed as follows:

$$\begin{aligned}
\mathcal{T}_p=&\frac{G_F}{\sqrt{2}}\sum_{p=u,c}V^*_{pq}V_{pb}[a_1^p(\overline{q}\gamma_\mu L u)\otimes(\overline{u}\gamma^\mu L b)+a_2^p(\overline{u}\gamma_\mu L u)\otimes(\overline{q}\gamma^\mu L b)+a_3^p(\overline{q'}\gamma_\mu L q')\otimes(\overline{q}\gamma^\mu L b)+a_4^p(\overline{q}\gamma_\mu L q')\\
&\otimes(\overline{q}\gamma'^{\mu}L b)+a_5^p(\overline{q'}\gamma_\mu R q')\otimes(\overline{q}\gamma^\mu L b)+a_6^p(-2)(\overline{q}R q')\otimes(\overline{q'}L b)+a_7^p\tfrac{3}{2}e_{q'}(\overline{q'}\gamma_\mu R q')\otimes(\overline{q}\gamma^\mu L b)\\
&+(-2)(a_8^p\tfrac{3}{2}e_{q'}+a_{8a})(\overline{q}R q')\otimes(\overline{q'}L b)+a_9^p\tfrac{3}{2}e_{q'}(\overline{q'}\gamma_\mu L q')\otimes(\overline{q}\gamma^\mu L b)+(a_{10}^p\tfrac{3}{2}e_{q'}+a_{10a}^p)(\overline{q}\gamma_\mu L q')\otimes(\overline{q'}\gamma^\mu L b)],
\end{aligned} \tag{5}$$

where the symbol $\otimes$ denotes $\langle M_1M_2|j_2\otimes j_1|B\rangle\equiv\langle M_2|j_2|0\rangle\langle M_1|j_1|B\rangle$. The effective a_i^p's which contain next-to-leading order (NLO) coefficients and $\mathcal{O}(\alpha_s)$ hard scattering corrections are found to be

$$a^c_{1,2}=0,\ \ a_i^c=a_i^u, \quad i=3,5,7,8,9,10,8a,10a, \tag{6}$$

$$a_1^u=C_1+\frac{C_2}{N}+\frac{\alpha_s}{4\pi}\frac{C_F}{N}C_2F_{M_2},$$

$$a_2^u=C_2+\frac{C_1}{N}+\frac{\alpha_s}{4\pi}\frac{C_F}{N}C_1F_{M_2},$$

$$a_3^u=C_3+\frac{C_4}{N}+\frac{\alpha_s}{4\pi}\frac{C_F}{N}C_4F_{M_2},$$

$$a_4^p=C_4+\frac{C_3}{N}+\frac{\alpha_s}{4\pi}\frac{C_F}{N}\left[C_3[F_{M_2}+G_{M_2}(s_q)+G_{M_2}(s_b)]+C_1G_{M_2}(s_p)+(C_4+C_6)\sum_{f=u}^{b}G_{M_2}(s_f)+C_gG_{M_2,g}\right],$$

$$a_5^u=C_5+\frac{C_6}{N}+\frac{\alpha_s}{4\pi}\frac{C_F}{N}C_6(-F_{M_2}-12),$$

$$a_6^p=C_6+\frac{C_5}{N}+\frac{\alpha_s}{4\pi}\frac{C_F}{N}\left[C_1G'_{M_2}(s_p)+C_3[G'_{M_2}(s_q)+G'_{M_2}(s_b)]+(C_4+C_6)\sum_{f=u}^{b}G'_{M_2,g}(s_f)+C_gG'_{M_2,g}\right],$$

$$a_7^u=C_7+\frac{C_8}{N}+\frac{\alpha_s}{4\pi}\frac{C_F}{N}C_8(-F_{M_2}-12),$$

$$a_8^p=C_8+\frac{C_7}{N},$$

$$a_{8a}^p=\frac{\alpha_s}{4\pi}\frac{C_F}{N}\left[(C_8+C_{10})\sum_{f=u}^{b}\frac{3}{2}e_fG'_{M_2}(s_f)+C_9\frac{3}{2}[e_qG'_{M_2}(s_q)+e_bG'_{M_2}(s_b)]\right],$$

$$a_9^u=C_9+\frac{C_{10}}{N}+\frac{\alpha_s}{4\pi}\frac{C_F}{N}C_{10}F_{M_2},$$

$$a_{10}^u=C_{10}+\frac{C_9}{N}+\frac{\alpha_s}{4\pi}\frac{C_F}{N}C_9F_{M_2},$$

$$a_{10a}^p=\frac{\alpha_s}{4\pi}\frac{C_F}{N}\left[(C_8+C_{10})\frac{3}{2}\sum_{f=u}^{b}e_fG_{M_2}(s_f)+C_9\frac{3}{2}[e_qG_{M_2}(s_q)+e_bG_{M_2}(s_b)]\right],$$

where $q=d,s$. $q'=u,d,s$ and $f=u,d,s,c,b$. $C_F=(N^2-1)/(2N)$ and $N=3$ is the number of colors. The internal quark mass in the penguin diagrams enters as $s_f=m_f^2/m_b^2$. $\bar{x}=1-x$ and $\bar{u}=1-u$:

$$F_{M_2}=-12\ln\frac{\mu}{m_b}-18+f_{M_2}^{\mathrm{I}}+f_{M_2}^{\mathrm{II}},\tag{7}$$

$$f_{M_2}^{\mathrm{I}}=\int_0^1 dx g(x)\phi_{M_2}(x),\quad g(x)=3\frac{1-2x}{1-x}\ln x-3i\pi,$$

$$f_{M_2}^{\mathrm{II}}=\frac{4\pi^2}{N}\frac{f_{M_1}f_B}{f_+^{B\to M_1}(0)M_B^2}\int_0^1 dz\frac{\phi_B(z)}{z}\times\int_0^1 dx\frac{\phi_{M_1}(x)}{x}\int_0^1 dy\frac{\phi_{M_2}(y)}{y},\tag{8}$$

$$G_{M_2,g}=-\int_0^1 dx\frac{2}{\bar{x}}\phi_{M_2}(x),\tag{9}$$

$$G_{M_2}(s_q)=\frac{2}{3}-\frac{4}{3}\ln\frac{\mu}{m_b}+4\int_0^1 dx\,\phi_{M_2}(x)\times\int_0^1 du\,u\bar{u}\ln[s_q-u\bar{u}\bar{x}-i\epsilon],\tag{10}$$

$$G'_{M_2,g}=-\int_0^1 dx\frac{3}{2}\phi_{M_2}^0(x)=-\frac{3}{2},\tag{11}$$

$$G'_{M_2}(s_q)=\frac{1}{3}-\ln\frac{\mu}{m_b}+3\int_0^1 dx\,\phi_{M_2}^0(x)\times\int_0^1 du\,u\bar{u}\ln[s_q-u\bar{u}\bar{x}-i\epsilon],\tag{12}$$

where $\phi(x)$ and $\phi^0(x)$ are the meson's leading-twist DA and twist-3 DA, respectively. It should be noted that we have included $\mathcal{O}(\alpha_s)$ corrections to a_6 in Eq. (6). Although the a_6 term in Eq. (5) is formally $1/M_b$ suppressed, it is chirally enhanced by $\mu_P = M_P^2/(m_q + m_{\bar{q}'})$ and known to be important to interpret the CELO [6] measurement. As a result the $\mathcal{O}(\alpha_s)$ correction to a_6 would be the most important one among the corrections to a_i. We see that there are logarithm terms $\ln \mu/m_b$ appearing in Eqs. (7)–(12), which is the result of one loop integration. If the scale μ is chosen to be small, the logarithm would be large and has to be resummed by using the renormalization group method. In this paper we choose $\mu = m_b$, then the logarithm disappeared and the resummation is not necessary. As a result, the effective coefficients a_i^p's are obtained to the order of $\alpha_s(m_b)$ corrections (see also in Ref. [7]).

We realize that the contribution of the strong penguins depicted in Figs. 1(e) and 1(f) to a_6 could be reliably estimated without IR divergence. As an example, we show the contribution of Fig. 1(f) in the following. With the assignment of the vertex $\delta_{\alpha\beta} i f_{M_2} \mu_{M_2} \gamma_5 \phi^0(x)/4N_c$ to M_2 and its constituents, we can get the hard amplitudes of Fig. 1(f) as

$$H_f \sim i f_{M_2} \mu_{M_2} \frac{\alpha_s}{4\pi} \frac{C_F}{N} \int_0^1 dx\, \phi^0(x) \frac{3(1-x) m_b^2}{k^2} \times \bar{q}_i \gamma_\mu (1-\gamma_5) b_i \sim \bar{q}_i \gamma_\mu (1-\gamma_5) b_i \int_0^1 dx\, \phi^0(x). \tag{13}$$

We can see that the end point IR divergence in $1/k^2$ $[k^2 = (1-x) m_b^2]$ is canceled by the term $(1-x)$ in the numerator and the amplitude is finite. For the amplitude of Fig. 1(e), it is easy to note that the denominator k^2 of the gluon propagator is canceled by the quark loop and the integration of $\int_0^1 dx G(s_f)$ is also finite itself. However, if all the external quarks are treated as free qurks at first, IR divergence will appear. In the case of free quarks, one can get the hard amplitudes of Fig. 1(f) as

$$\begin{aligned} H_f &\sim \frac{m_b^2}{k^2} \bar{d}_i \gamma_\mu (1-\gamma_5) b_j \bar{q}_j \gamma^\mu q_i \\ &\sim \frac{m_b^2}{k^2} [\bar{d}_i \gamma_\mu (1-\gamma_5) b_j \bar{q}_j \gamma^\mu (1-\gamma_5) q_i + \bar{d}_i \gamma_\mu \\ &\quad \times (1-\gamma_5) b_j \bar{q}_j \gamma^\mu (1+\gamma_5) q_i]. \end{aligned} \tag{14}$$

At this stage the quark pair $\bar{q}d$ is in color-singlet configuration. After Fierz rearrangement, one gets

$$\begin{aligned} H_f \sim \frac{m_b^2}{k^2} [&\bar{d}_i \gamma_\mu (1-\gamma_5) q_i \otimes \bar{q}_j \gamma^\mu (1-\gamma_5) b_j \\ &- 2 \bar{d}_i (1+\gamma_5) q_i \otimes \bar{q}_j (1-\gamma_5) b_j]. \end{aligned} \tag{15}$$

From the above equation we can see that Fig. 1(f) contributes to a_4 and a_6 equally and its contribution is IR divergent when $k^2 \to 0$ in free quark approach. Phenomenologically, one may have to treat k^2 as a parameter. In the framework employed here, the virtuality of the gluon is convoluted with the meson's DA. Furthermore, The NLO strong penguin contributions to a_4 and a_6 terms are different.

Finally, the chirally enhanced contributions from Figs. 1(g) and 1(h) to a_6 are canceled when they are summed up. One can easily see this cancellation by putting both the leading-twist DA and twist-3 DA $\phi(x)$ and $\phi^0(x)$ to Figs. 1(g) and 1(h) and calculating these two diagrams. Because $\phi^0(x)$ gives the chirally enhanced contributions, one can easily see that these contributions are canceled.

With Eqs. (5) and (6), we can write down the amplitudes of $B \to \pi\pi$ and $K\pi$ decays

$$\begin{aligned} \mathcal{M}(\bar{B}_d^0 \to \pi^+ \pi^-) = \frac{G_F}{\sqrt{2}} i f_\pi (M_B^2 - M_\pi^2) F^{B\to\pi}(0) |\lambda V_{cb}| \{ &R_b e^{-i\gamma} [a_1^u + a_4^u + a_{10}^u + a_{10a}^u + R_{\pi^-}(a_6^u + a_8^u + a_{8a})] \\ &- [a_4^c + a_{10}^c + a_{10a}^c + R_\pi (a_6^c + a_8^c + a_{8a})] \}, \end{aligned} \tag{16}$$

$$\begin{aligned} \mathcal{M}(\bar{B}_d^0 \to \pi^0 \pi^0) = \frac{G_F}{\sqrt{2}} i f_\pi (M_B^2 - M_\pi^2) F^{B\to\pi}(0) |\lambda V_{cb}| \\ \times \left\{ R_b e^{-i\gamma} \left[-a_2^u + a_4^u + \frac{3}{2} a_7^u - \frac{3}{2} a_9^u - \frac{1}{2} a_{10}^u + a_{10a}^u + R_{\pi^0} \left(a_6^u - \frac{1}{2} a_8^u + a_{8a} \right) \right] \right. \\ \left. - \left[a_4^c + \frac{3}{2} a_7^c - \frac{3}{2} a_9^c - \frac{1}{2} a_{10}^c + a_{10a}^c + R_{\pi^0} \left(a_6^c - \frac{1}{2} a_8^c + a_{8a} \right) \right] \right\}, \end{aligned} \tag{17}$$

$$\begin{aligned} \mathcal{M}(B_u^- \to \pi^0 \pi^-) = \frac{G_F}{2} i f_\pi (M_B^2 - M_\pi^2) F^{B\to\pi}(0) |\lambda V_{cb}| \left\{ R_b e^{-i\gamma} \left[a_1^u + a_2^u + \frac{3}{2} (-a_7^u + R_\pi a_8^u + a_9^u + a_{10}^2) \right] \right. \\ \left. - \frac{3}{2} [-a_7^c + R_{\pi^0} a_8^c + a_9^c + a_{10}^c)] \right\}, \end{aligned} \tag{18}$$

$$\mathcal{M}(\overline{B}_d^0\to\overline{K}^0\pi^0)=\frac{G_F}{2}if_\pi(M_B^2-M_K^2)F^{B\to K}(0)(1-\lambda^2)|V_{cb}|\left\{R_b' e^{-i\gamma}\left[a_2^u-\frac{3}{2}(a_7^u-a_9^u)\right]-\frac{3}{2}(a_7^u-a_9^u)\right\}$$
$$-\frac{G_F}{2}if_K(M_B^2-M_\pi^2)F^{B\to\pi}(0)(1-\lambda^2)|V_{cb}|\left\{R_b' e^{-i\gamma}\left[-a_4^u-R_K\left(a_6^u-\frac{1}{2}a_8^u+a_{8a}\right)+\frac{1}{2}a_{10}^u-a_{10a}^u\right]\right.$$
$$\left.+\left[-a_4^c-R_K\left(a_6^c-\frac{1}{2}a_8^c+a_{8a}\right)+\frac{1}{2}a_{10}^c-a_{10a}^c\right]\right\}, \tag{19}$$

$$\mathcal{M}(\overline{B}_d^0\to K^-\pi^+)=\frac{G_F}{\sqrt{2}}if_\pi(M_B^2-M_K^2)F^{B\to K}(0)(1-\lambda^2)|V_{cb}|\{R_b' e^{-i\gamma}[a_1^u+a_4^u+R_K(a_6^u+a_8^u+a_{8a})+a_{10}^u+a_{10a}^u]$$
$$\times[a_4^c+R_K(a_6^c+a_8^c)+a_{10}^c+a_{10a}^c]\}, \tag{20}$$

$$\mathcal{M}(\overline{B}_u^-\to K^-\pi^0)=\frac{G_F}{2}if_K(M_B^2-M_\pi^2)F^{B\to\pi}(0)(1-\lambda^2)|V_{cb}|\{R_b' e^{-i\gamma}[a_1^u+a_4^u+R_K(a_6^u+a_8^u+a_{8a})+a_{10}^u+a_{10a}^u]$$
$$\times[a_4^c+R_K(a_6^c+a_8^c+a_{8a})+a_{10}^c+a_{10a}^c]\}+\frac{G_F}{2}if_\pi(M_B^2-M_K^2)F^{B\to K}(0)\left(1-\frac{\lambda^2}{2}\right)|V_{cb}|$$
$$\times\left\{R_b' e^{-i\gamma}\left[a_2^u+\frac{3}{2}(a_9^u-a_7^u)\right]+\frac{3}{2}(a_9^c-a_7^c)\right\}, \tag{21}$$

$$\mathcal{M}(\overline{B}_u^-\to\overline{K}^0\pi^-)=\frac{G_F}{\sqrt{2}}if_K(M_B^2-M_\pi^2)F^{B\to\pi}(0)\left(1-\frac{\lambda^2}{2}\right)|V_{cb}|\left\{R_b' e^{-i\gamma}\left[a_4^u+R_K\left(a_6^u-\frac{1}{2}a_8^u+a_{8a}\right)-\frac{1}{2}a_{10}^u+a_{10a}^u\right]\right.$$
$$\left.+\left[a_4^c++R_K\left(a_6^c-\frac{1}{2}a_8^c+a_{8a}\right)-\frac{1}{2}a_{10}^c+a_{10a}^c\right]\right\}, \tag{22}$$

where

$$R_b=\frac{1-\lambda^2/2}{\lambda}\left|\frac{V_{ub}}{V_{cb}}\right|$$

and

$$R_b'=\frac{\lambda}{1-\lambda^2/2}\left|\frac{V_{ub}}{V_{cb}}\right|.$$

V_{cb}, V_{ud}, and V_{us} are chosen to be real and γ is the phase of V_{ub}^*. $\lambda=|V_{us}|=0.2196$. $R_P=2\mu_P$.

III. NUMERICAL CALCULATIONS AND DISCUSSIONS OF RESULTS

In the numerical calculations we use [8]

$$f_\pi=0.133\ \text{GeV},\quad f_K=0.158\ \text{GeV},$$
$$f_B=0.180\ \text{GeV},$$
$$\tau(B^+)=1.65\times10^{-12}\ \text{s},\quad \tau(B^0)=1.56\times10^{-12}\ \text{s},$$
$$M_B=5.2792\ \text{GeV},\quad M_b=4.8\ \text{GeV},$$
$$M_c=1.4\ \text{GeV},$$
$$m_u=4.0\ \text{MeV},\quad M_d=9.0\ \text{MeV},$$
$$M_s=80\ \text{MeV}.$$

For the leading-twist DA $\phi(x)$ and the twist-3 DA $\phi^0(x)$ of K and π, we use the well known asymptotic form of these DA [9,10]

$$\phi_{\pi,K}(x)=6x(1-x),\quad \phi^0_{\pi,K}(x)=1. \tag{23}$$

For B meson, the wave function is chosen as that used in Refs. [11,12]

$$\phi_B(x)=N_B x^2(1-x)^2\exp\left[-\frac{M_B^2x^2}{2\omega_B^2}\right], \tag{24}$$

with $\omega_B=0.4$ GeV, and N_B is the normalization constant to make $\int_0^1 dx\,\phi_B(x)=1$. Here the decay constant in the wave function has been factored out. So the wave function can be normalized to 1. It is also necessary to note that $\phi_B(x)$ is strongly peaked around $x=0.1$. This character is consistent

TABLE I. The QCD coefficients a_i^p at NLO for renormalization scale $\mu = m_b$ (in units of 10^{-4} for $a_3, \ldots, a_{10}$). Results from different references are shown for comparison.

	ours	[4]	[13]	[14]
a_1	$1.042+0.014i$	$1.038+0.018i$	1.05	1.46
a_2	$0.046-0.082i$	$0.082-0.080i$	0.053	0.24
a_3	$65.2+26.8i$	$40+20i$	48	72
a_4^u	$-314-152i$	$-290–150i$	$-439-77i$	$-383-121i$
a_4^c	$-370\text{-}54i$	$-340\text{-}80i$		
a_5	$-55.7–31.4i$	$-50\text{-}20i$	-45	-27
a_6^u	$-380+(-46–106i)$	-380	$-575–77i$	$-435–121i$
a_6^c	$-380+(-71–41i)$	-380		
a_7	$1.25+0.3i$		$0.5–1.3i$	$-0.89–2.73i$
a_8	$3.8+(-0.1–0.5i)$		$4.6–0.4i$	$3.3–0.91i$
a_9	$-98.4+1.47I$		$-94–1.3i$	$-93.9–2.7i$
a_{10}	$-39.3+7.23i$		$-14–0.4i$	$0.32–0.90i$

with the observation of heavy quark effective theory that the wave function should be peaked around $\Lambda_{\rm QCD}/M_B$. With such choice, we find

$$\int_0^1 dx \frac{\phi_B(x)}{x} = 11.15, \tag{25}$$

which is near to the argument [4] in which $\int_0^1 dx\, \phi_B(x)/x = M_B/\lambda_B = 17.56$ with $\lambda_B = 0.3$ GeV. We have used the unitarity of the Cabibbo-Kobayashi-Maskawa (CKM) matrix $V_{uq}^* V_{ub} + V_{cq}^* V_{cb} + V_{tq}^* V_{tb} = 0$ to decompose the amplitudes into terms containing $V_{uq}^* V_{ub}$ and $V_{cq}^* V_{cb}$, and

$$|V_{ud}| = 1 - \lambda^2/2,\ \ |V_{ub}/V_{cb}| = 0.085 \pm 0.02 \tag{26}$$
$$|V_{cb}| = 0.0395 \pm 0.0017,\ \ |V_{us}| = \lambda = 0.2196.$$

We leave the CKM angle γ as a free parameter. For the form factors, we use $F^{B\to\pi}(0) = 0.3$ and $F^{B\to K}(0) = 1.13 F^{B\to\pi}(0)$.

Numerical values for $a_i^p(\pi\pi)$ and $a_i^p(\pi K)$ are presented in Table I. It should be noted that $a_i(K\pi)$ are generally different to $a_i(\pi\pi)$ and also change from case to case due to $f_{M_2}^{\rm II}$ in the formulas of a_i, where M_2 could be K or π. However, with our choice of parameters

$$\frac{f_\pi}{F^{B\to\pi}(0)} \simeq \frac{f_K}{F^{B\to K}(0)}, \tag{27}$$

and the same DAs $\phi_{K,\pi}(x)$, the $a_i(K\pi) \simeq a_i(\pi\pi)$. From Table I, we can find that all a_i^p develop strong phases due to hard strong scattering. Our a_2 is very different from that of [13,14] in both real and imaginary part because of the contribution of Figs. 1(g) and 1(h). So, theoretical predictions for the decays dominated by a_2 may be very different between naive factorization approach and QCD improved factorization approach. Numerically, we find that the $\mathcal{O}(\alpha_s)$ strong penguin contributions which collected in a_4 and a_6 are small because of the large cancellation between Figs. 1(e) and 1(f). In detail, the strong penguin contributions to a_4 and a_6 are

$$\begin{aligned} a^p_{4\ \rm pen} &= \frac{\alpha_s}{4\pi}\frac{C_F}{N}\Bigg[C_1 G_{M_2}(s_p) + C_3[G_{M_2}(s_q) + G_{M_2}(s_b)] \\ &\quad + (C_4 + C_6)\sum_{f=u}^{b} G_{M_2}(s_f) + C_g G_{M_2,g}\Bigg] \\ &= \frac{\alpha_s}{4\pi}\frac{C_F}{N}\times\begin{cases} (-0.780 - 1.744i) + (0.858), & p=u, \\ (-1.473 - 0.529i) + (0.858), & p=c, \end{cases} \end{aligned} \tag{28}$$

$$\begin{aligned} a^p_{6\ \rm pen} &= \frac{\alpha_s}{4\pi}\frac{C_F}{N}\Bigg[C_1 G'_{M_2}(s_p) + C_3[G'M_2(s_q) + G'_{M_2}(s_b)] \\ &\quad + (C_4 + C_6)\sum_{f=u}^{b} G'_{M_2}(s_f) + C_g G'_{M_2,g}\Bigg] \\ &= \frac{\alpha_s}{4\pi}\frac{C_F}{N}\times\begin{cases} (-0.780 - 1.299i) + (0.2145), & p=u, \\ (-1.095 - 0.510i) + (0.2145), & p=c, \end{cases} \end{aligned} \tag{29}$$

where the numbers in the brackets are the contributions of Figs. 1(e) and 1(f), respectively. The cancellation in a_6 is weaker than that in a_4, since the contribution of Fig. 1(f) to a_6 is small. The other diagrams will dominate the $\mathcal{O}(\alpha_s)$ hard scattering amplitudes.

Now it is time to discuss branching ratios and CP asymmetries of $B \to K\pi$ and $B \to \pi\pi$ in the QCD improved factorization approach. The branching ratio is given by

$$\mathrm{Br}(B \to K\pi, \pi\pi) = \tau_B/(16\pi m_B) |\mathcal{M}(B \to K\pi, \pi\pi)|^2 s, \tag{30}$$

where $s = 1/2$ for $B \to \pi^0\pi^0$ mode, and $s = 1$ for the other decay modes. For the charged B meson decays, the direct CP asymmetry parameter is defined as

$$A_{CP}^{\rm dir} = \frac{|\mathcal{M}(B^+ \to f)|^2 - |\mathcal{M}(B^- \to \overline{f})|^2}{|\mathcal{M}(B^+ \to f)|^2 + |\mathcal{M}(B^- \to \overline{f})|^2}. \tag{31}$$

For the neutral B decaying into CP eigenstate f, i.e., $f = \overline{f}$, the effects of B^0-$\overline{B}^0$ mixing should be taken into account in studying CP asymmetry. Thus the CP asymmetry is time dependent, which is given by [15]

$$A_{CP}(t) = A_{CP}^{\rm dir}\cos(\Delta m t) - \frac{2\,\mathrm{Im}(\lambda_{CP})}{1 + |\lambda_{CP}|^2}\sin(\Delta m t), \tag{32}$$

where Δm is the mass difference of the two mass eigenstates of neutral B mesons, and A_{CP}^{dir} is the direct CP asymmetry defined in Eq. (31) with replacement of $B^+\to B^0$ and $B^-\to\overline{B}^0$, respectively. The parameter λ_{CP} is given by

$$\lambda_{CP}=\frac{V_{tb}^*V_{td}\langle f|H_{\mathrm{eff}}|\overline{B^0}\rangle}{V_{tb}V_{td}^*\langle f|H_{\mathrm{eff}}|B^0\rangle}. \tag{33}$$

With the above parameters and formulas, we get the branching ratios

$$\begin{aligned}
\mathrm{Br}(\overline{B}_d^0\to\pi^+\pi^-)&=7.55\times10^{-6}|e^{-i\gamma}+0.18e^{i8.0°}|^2,\\
\mathrm{Br}(\overline{B}_d^0\to\pi^0\pi^0)&=4.3\times10^{-8}|e^{-i\gamma}+1.19e^{-i132°}|^2,\\
\mathrm{Br}(B_u^-\to\pi^0\pi^-)&=4.73\times10^{-6}|e^{-i\gamma}+0.05e^{-i0.1°}|^2,\\
\mathrm{Br}(\overline{B}_d^0\to\overline{K}^0\pi^0)&=4.06\times10^{-9}|e^{-i\gamma}+31.9e^{i34°}|^2,
\end{aligned}\tag{34}$$

$$\begin{aligned}
\mathrm{Br}(\overline{B}_d^0\to K^-\pi^+)&=5.12\times10^{-7}|e^{-i\gamma}+5.23e^{-i172°}|^2,\\
\mathrm{Br}(B_u^-\to K^-\pi^0)&=2.91\times10^{-7}|e^{-i\gamma}+5.78e^{-i168°}|^2,\\
\mathrm{Br}(B_u^-\to\overline{K}^0\pi^-)&=4.08\times10^{-9}|e^{-i\gamma}+55.1e^{-i11.3°}|^2.
\end{aligned}$$

If we generally express Eq. (34) as $\mathrm{Br}=A(e^{-i\gamma}+ae^{-i\delta})$, then the direct CP asymmetry in Eq. (31) can be relevantly expressed as

$$A_{CP}^{\mathrm{dir}}=\frac{2a\sin\gamma}{1+a^2+2a\cos\delta\cos\gamma}. \tag{35}$$

Using the above equation, the numerical results for the direct CP asymmetry are obtained

$$\begin{aligned}
A_{CP}^{\mathrm{dir}}(B\to\pi^+\pi^-)&=\frac{5.0\%}{1.03+0.36\cos\gamma}\sin\gamma,\\
A_{CP}^{\mathrm{dir}}(B\to\pi^0\pi^0)&=-\frac{1.77}{2.42-1.59\cos\gamma}\sin\gamma,\\
A_{CP}^{\mathrm{dir}}(B\to\pi^0\pi^\mp)&=-1.7\times10^{-4}\sin\gamma,\\
A_{CP}^{\mathrm{dir}}(B\to K^0\pi^0)&=3.5\%\sin\gamma,\\
A_{CP}^{\mathrm{dir}}(B\to K^\mp\pi^\pm)&=-\frac{1.46}{28.4-10.4\cos\gamma}\sin\gamma,\\
A_{CP}^{\mathrm{dir}}(B\to K^\mp\pi^0)&=-\frac{2.40}{34.4-11.3\cos\gamma}\sin\gamma,\\
A_{CP}^{\mathrm{dir}}(B\to K^0\pi^\mp)&=-0.7\%\sin\gamma.
\end{aligned}\tag{36}$$

As is shown in Eq. (34), the strong phases are different by decay channels. We can also see from Eq. (36) that the direct CP violation in $B\to\pi^0\pi^\mp$ is neglectably small. The direct CP violation in $B\to\pi^+\pi^-$, $\pi^0K^\mp$, $K^0\pi^0$, $K^\mp\pi^0$, and $K^\mp\pi^\pm$ are only at a few percentage levels. The large CP violation effect may be expected in $B\to\pi^0\pi^0$ decays. However, it would remain undetectable before the running of the next generation B factories, for example, the CERN Large Hadron Collider (LHCB), due to its very small branching ratios ($\sim10^{-7}$) and its two neutral final states.

Recently, the CLEO Collaboration made the first observation of the decay modes $B\to\pi^+\pi^-$, $B\to K^0\pi^0$, and $B\to K^\pm\pi^0$ and also updated the decay modes $B\to K^\pm\pi^\mp$ and $B\to K^0\pi^\pm$ as follows [6]:

$$\begin{aligned}
\mathrm{Br}(B_d\to\pi^+\pi^-)&=(4.3^{+1.6}_{-1.4}\pm0.5)\times10^{-6},\\
\mathrm{Br}(B_u\to\pi^0\pi^\pm)&<12.7\times10^{-6},\\
\mathrm{Br}(B_d\to K^0\pi^0)&=(14.6^{+5.9+2.4}_{-5.1-3.3})\times10^{-6},\\
\mathrm{Br}(B_d\to K^\pm\pi^\mp)&=(17.2^{+2.5}_{-2.4}\pm1.2)\times10^{-6},\\
\mathrm{Br}(B_u\to K^\pm\pi^0)&=(11.6^{+3.0+1.4}_{-2.7-1.3})\times10^{-6},\\
\mathrm{Br}(B_u\to K^0\pi^\pm)&=(18.2^{+4.6}_{-4.0}\pm1.6)\times10^{-6}.
\end{aligned}\tag{37}$$

To compare with the data, we plot the CP averaged branching ratios for those modes as a function of γ in Fig. 2. Our results are plotted as curves and the CELO data are displayed as horizontal lines (thicker lines for center value, thin lines represent error bars at 2σ level). The horizontal line in Fig. 2 is the upper limit of the decay mode.

We find that the observed branching ratios of those decay modes can be well accommodated within the QCD improved factorization approach of Ref. [4] except the decay mode $B\to K^0\pi^0$. As shown in Eq. (19), the first term with $F^{B\to K}$ and the second term with $F^{B\to\pi}$ are *disconstructive*, which reduces the amplitude of $M(B\to K^0\pi^0)$ much smaller than that of other $B\to\pi K$ decays. As it is argued in Refs. [4,16], in the present theoretical framework, the final state interactions are computable and identical to the imaginary part of the amplitude which is generated by the hard scattering amplitudes. In this paper, we find the strong phase appears not large enough to change the two subamplitudes of $M(B\to K^0\pi^0)$ to be *constructive*. Our results agree with that in Refs. [13,17–19] where the decay rate of $B\to K^0\pi^0$ is also estimated to be small.

The CLEO observations have motivated many theoretical studies of those decay modes using different approaches [11,12,17,18,20]. In Refs. [18,21,22], it is suggested that $\gamma>90°$ is required to interpret the CLEO data. However, the global CKM fit has given the constraint $\gamma<90°$ at 99.6% C.L. [23]. The comparison between our results and CLEO data [6] implies $120°<\gamma<240°$ which arises from the constraint by $\mathrm{Br}(B\to\pi^-\pi^+)$. The observed $\mathrm{Br}(B\to\pi^-\pi^+)$ is smaller than many theoretical expectations. Negative $\cos\gamma$ is needed to suppress the theoretical estimations as it is suggested in Ref. [18]. The decay rate of $B\to\pi^-\pi^+$ can be also suppressed by using smaller form factor $F^{B\to\pi}(0)$ and/or smaller $|V_{ub}/V_{cb}|$. However, it would be very hard to ac-

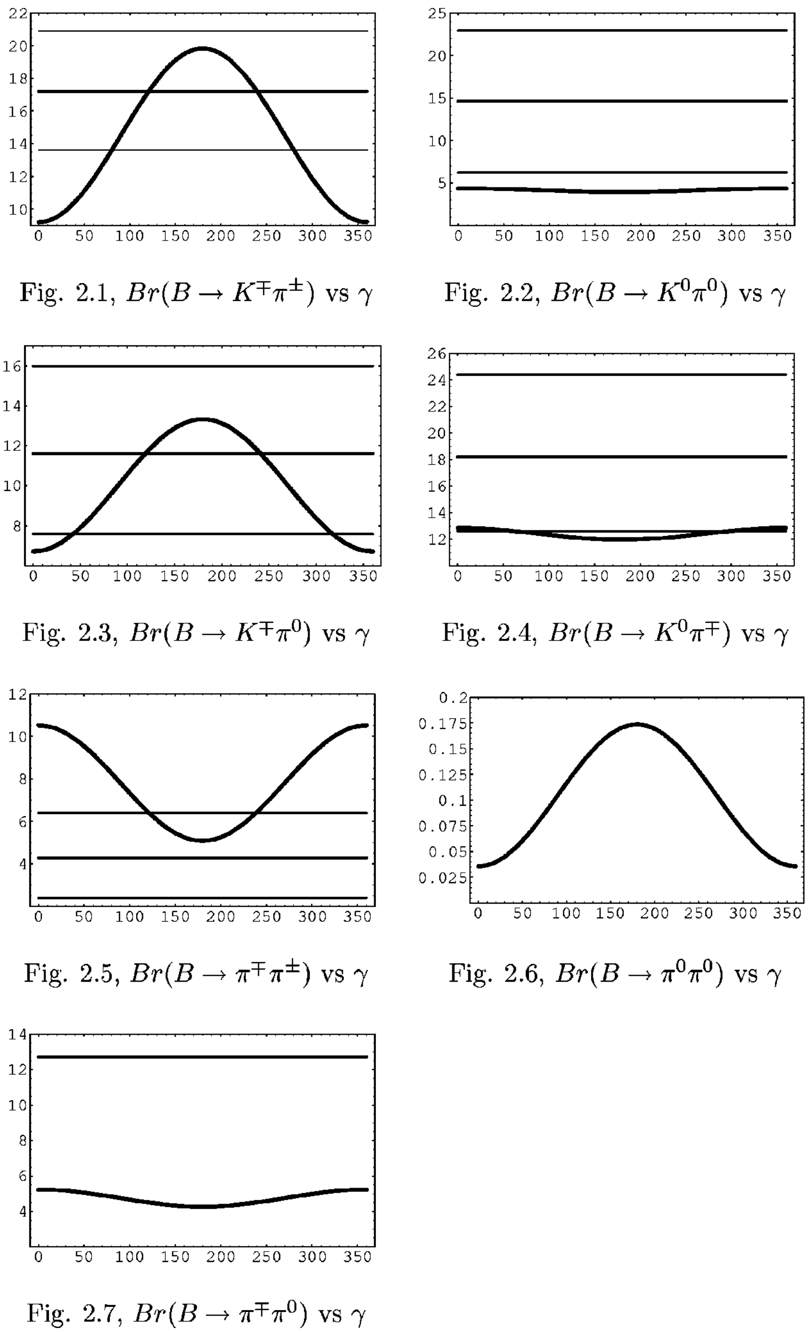

FIG. 2. CP-averaged Br($B\to\pi\pi,K\pi$) as a function of γ are shown as curves for $F^{B\to\pi}=0.3$ and $|V_{ub}/V_{cb}|=0.08$ (in units of 10^{-6}). The branching ratios measured by CLEO Collaboration are shown by horizontal solid lines. The thicker solid lines are its center values, thin lines are its error bars or the upper limit.

count for the large decay rates of $B\to K\pi$ modes in this case. For those reasons, it might be difficult to solve the controversy between the global CKM fit and the model-dependent constraints from the charmless decays $B\to K\pi,\pi\pi$ within the QCD improved factorization approach.

IV. SUMMARY

We have studied $B\to K^{\mp}\pi^{\pm}$, $B\to K^{0}\pi^{0}$, $B\to K^{\mp}\pi^{0}$, $B\to K^{0}\pi^{\mp}$, $B\to\pi^{\mp}\pi^{\pm}$, $B\to\pi^{0}\pi^{0}$, and $B\to\pi^{\mp}\pi^{0}$ decays, in a QCD improved factorization approach.

The strong penguin contributions [Figs. 1(e),1(f)] are discussed in detail and found to be small because of the cancellations between them. The most important power corrections to these chiral enhanced terms (i.e., a_6) are identified and found to be free of infrared divergence. With the choice of twist-3 DA $\phi_p^0(x)=1$, the a_6 gets a large imaginary part and its real part is enhanced by 10–20 %. The other NLO coefficients a_i also acquire complex phases from the hard scattering as depicted by Figs. 1(a)–1(e) which are shown by the function $g(x)$ and $G(s,x)$ in Eq. (12). We can see that $g(x)$ is a new source of strong phase in addition to $G(s,x)$ of the well known BSS mechanism [24]. Compared to the naive factorization, the strong phases are estimated reliably without the arbitrariness of gluon virtuality k^2 within the QCD improved factorization formalism [4]. The strong phase due to the hard scattering in the decay modes are found to vary from $0°$ to $172°$, depending on the decay mode. In the decays $B\to\pi^{0}\pi^{0}$, $K^{\pm}\pi^{\mp}$, and $K^{\pm}\pi^{0}$, the strong phase are found to be as large as $100°<\delta<180°$. In other decay modes, the strong phases are rather small.

The predicted branching ratios of $B \to \pi K$ and $B \to \pi^{\mp}\pi^{\pm}$ decay modes are in good agreement with the experimental measurement by the CLEO Collaboration except for the decay $B \to K^0\pi^0$. The most serious constraint on the weak angle γ comes from the small experimental value of $\mathrm{Br}(B \to \pi^-\pi^+)$ which implies $120° < \gamma < 240°$. We found that it is hard to solve the controversy between the constraints on γ from the global CKM fit and the estimations of the charmless decays $B \to K\pi, \pi\pi$. The CP violation effects in $B \to \pi^0\pi^{\mp}$ is neglectably small. The direct CP violation effects in $B \to \pi^+\pi^-$, $\pi^0 K^{\mp}$, $K^0\pi^0$, $K^{\mp}\pi^0$, and $K^{\mp}\pi^{\pm}$ are only at a few percentage level. The large CP violation effect may be expected in $B \to \pi^0\pi^0$ decays.

Note added. After finishing this work, we found that Ref. [25] also discussed $B \to K\pi$ and $\pi\pi$ decays with a similar method, and Ref. [26] compared different approaches.

Note added in proof. After this paper was submitted, the BARBAR Collaboration reported their measurement of branching ratios for charmless B decays to charged pions and kions [27]: $B(B^0 \to \pi^{\pm}\pi^{\mp}) = (9.3^{+2.6+1.2}_{-2.3-1.4}) \times 10^{-6}$ and $B(B^0 \to K^{\pm}\pi^{\pm}) = (12.5^{+3,0+1,3}_{-2.6-1.7}) \times 10^{-6}$. Our predictions agree with the BARBAR data very well. We note that *positive* $\cos\gamma$ is favored if the BARBAR data are taken as a guide.

ACKNOWLEDGMENTS

We acknowledge the Grant-in-Aid for Scientific Research on Priority Areas (Physics of CP violation with Contract Nos. 09246105 and 1014028). Y.D.Y. and M.Z.Y. thank JSPS for support.

[1] M. Bauer, B. Stech, and M. Wirbel, Z. Phys. C **29**, 637 (1985); **34**, 103 (1987).
[2] D. Zeppenfield, Z. Phys. C **8**, 77 (1981); L.L. Chau, Phys. Rev. D **43**, 2176 (1991).
[3] M. Gronau, J. Rosner, and D. London, Phys. Rev. Lett. **73**, 21 (1994).
[4] M. Beneke, G. Buchalla, M. Neubert, and C.T. Sachrajda, Phys. Rev. Lett. **83**, 1914 (1999).
[5] For a review, see G. Buchalla, A.J. Buras, and M.E. Lautenbacher, Rev. Mod. Phys. **68**, 1125 (1996).
[6] CLEO Collaboration, D. Cronin-Hennessy *et al.*, hep-ex/0001010.
[7] R. Fleischer, Z. Phys. C **58**, 483 (1993).
[8] Particle Data Group, C. Caso *et al.*, Eur. Phys. J. C **3**, 1 (1998).
[9] V.L. Chernyak and A.R. Zhitinissky, Phys. Rep. **112**, 173 (1983).
[10] V.M. Braun and I.E. Filyanov, Z. Phys. C **48**, 239 (1990).
[11] Y.Y. Keum, H.-n. Li, and A.I. Sanda, Report No. KEK-TH-642, NCKU-HEP-00-01, hep-ph/0004004; Report No. NCKU-HEP-00-02, DPNU-00-14, hep-ph/0004173.
[12] C.D. Lü, K. Ukai, and M. Z. Yang, Report No. HUPD-9924, DPNU-00-15, hep-ph/004213.
[13] A. Ali, G. Kramer, and C.D. Lü, Phys. Rev. D **58**, 094009 (1998).
[14] Y.-H. Chen, H.-Y. Cheng, B. Tseng, and K.-C. Yang, Phys. Rev. D **60**, 094014 (1999).
[15] M. Gronau, Phys. Rev. Lett. **63**, 1451 (1989).
[16] M. Beneke, Report No. CERN-TH/99-319, hep-ph/9910505.
[17] H.Y. Cheng, Phys. Lett. B **335**, 428 (1994); **395**, 345 (1997); H.Y. Cheng and B. Tseng, Phys. Rev. D **58**, 094005 (1998); Y.H. Chen, H.Y. Cheng, and B. Tseng, *ibid.* **59**, 074003 (1999).
[18] W.S. Hou and K.C. Yang, Phys. Rev. D **61**, 073014 (2000); Phys. Rev. Lett. **84**, 4806 (2000); W.S. Hou, J.G. Smith, and F. Würthwein, hep-ex/9910014.
[19] H.-Y. Cheng and K.-C. Yang, Phys. Rev. D **62**, 054029 (2000).
[20] M. Gronau and J.L. Rosner, Phys. Rev. D **61**, 073008 (2000); **59**, 113002 (1999).
[21] N.G. Deshpande *et al.*, Phys. Rev. Lett. **82**, 2240 (1999).
[22] X.G. He, W.S. Hou, and K.C. Yang, Phys. Rev. Lett. **83**, 1100 (1999).
[23] F. Caravaglios, F. Parodi, P. Roudeau, and A. Stocchi, Report No. LAL 00-04, hep-ph/0002171.
[24] M. Bander, D. Silverman, and A. Soni, Phys. Rev. Lett. **43**, 242 (1979).
[25] D. Du, D. Yang, and G. Zhu, Phys. Lett. B **488**, 46 (2000).
[26] Y.Y. Keum and H.N. Li, hep-ph/0006001.
[27] BARBAR Collaboration, B. Aubert *et al.*, BARBAR-CONF-00/14, SLAC-PUB-8536.